THE JOURNAL OF BIOLOGICAL CHEMISTRY VOL. 281, NO. 6, pp. 3127–3136, February 10, 2006

A Conserved Histidine-Aspartate Pair Is Required for Exovinyl Reduction of Biliverdin by a Cyanobacterial Phycocyanobilin:Ferredoxin Oxidoreductase*

Received for publication, September 14, 2005, and in revised form, November 28, 2005 Published, JBC Papers in Press, December 2, 2005, DOI 10.1074/jbc.M510126200

Shih-Long Tu[‡], **Wesley Sughrue**[§], **R. David Britt**[§], **and J. Clark Lagarias**[‡1]

From the [‡]*Section of Molecular and Cellular Biology, College of Biological Sciences and the* [§]*Department of Chemistry, University of California, Davis, California 95616*

Phycocyanobilin:ferredoxin oxidoreductase is a member of the ferredoxin-dependent bilin reductase family and catalyzes two vinyl reductions of biliverdin IXα to produce phycocyanobilin, the pigment precursor of both phytochrome and phycobiliprotein chromophores in cyanobacteria. Atypically for ferredoxin-dependent enzymes, phycocyanobilin:ferredoxin oxidoreductase mediates direct electron transfers from reduced ferredoxin to its tetrapyrrole substrate without metal ion or organic cofactors. We previously showed that bound bilin radical intermediates could be detected by low temperature electron paramagnetic resonance and absorption spectroscopies (Tu, S., Gunn, A., Toney, M. D., Britt, R. D., and Lagarias, J. C. (2004) *J. Am. Chem. Soc.* 126, 8682–8693). On the basis of these studies, a mechanism involving sequential electron-coupled proton transfers to protonated bilin substrates buried within the phycocyanobilin:ferredoxin oxidoreductase protein scaffold was proposed. The present investigation was undertaken to identify catalytic residues in phycocyanobilin:ferredoxin oxidoreductase from the cyanobacterium *Nostoc* sp. PCC7120 through site-specific chemical modification and mutagenesis of candidate proton-donating residues. These studies identified conserved histidine and aspartate residues essential for the catalytic activity of phycocyanobilin:ferredoxin oxidoreductase. Spectroscopic evidence for the formation of stable enzyme-bound biliverdin radicals for the H85Q and D102N mutants support their role as a "coupled" proton-donating pair during the reduction of the biliverdin exovinyl group.

Ferredoxin-dependent bilin reductases (FDBRs)[2] are a family of enzymes involved in the biosynthesis of linear tetrapyrrole chromophore (bilin) precursors of the light-harvesting phycobiliproteins and the light-sensing phytochromes (1, 2). The diverse bilin products synthesized by FDBRs contribute to the broad range of light absorption of phycobiliprotein antennae throughout the visible and near-infrared spectrum (3). Widely distributed in oxygenic photosynthetic organisms, FDBRs catalyze the reduction of heme- and chlorophyll-derived oxidation products by targeting different double bonds within their bilin substrates (2, 4).

Phycocyanobilin:ferredoxin oxidoreductase (PcyA, EC 1.3.7.5) is an atypical FDBR, catalyzing reduction of both vinyl groups of biliverdin IXα (BV) to produce 3Z/3E phycocyanobilin (3Z/3E-PCB) (2). More recent studies indicate that the first stable intermediate is 18^1,18^2-dihydrobiliverdin (18^1,18^2-DHBV), demonstrating that reduction of the D-ring exovinyl group precedes reduction of the A-ring endovinyl group (Fig. 1) (5). Based on the lack of a metal/organic cofactor and on low temperature electron paramagnetic resonance (EPR) spectroscopy, we proposed a radical mechanism for PcyA (6). As depicted in Fig. 1, the interconversion of BV to PCB formally involves a series of ferredoxin-mediated one-electron transfers to the PcyA-bound bilin substrate that require the participation of up to five proton-donating residues within the enzyme. Our investigations also provided spectroscopic evidence for two vinyl radical intermediates, each of which exists as a mixture of protonated neutral and deprotonated anionic species (6).

Substrate protonation by enzymes requires ionizable residues and/or tightly bound water/cofactors within their active sites. Multiple sequence alignment reveals numerous conserved residues in the extended FDBR family. As shown in Fig. 2, such residues cluster within two highly conserved regions of these enzymes (Fig. 2, *Box 1* and *2*). Ionizable residues conserved in all FDBRs include aspartate 116 (Asp^{116}), aspartate 217 (Asp^{217}), and tyrosine 209 (Tyr^{209})[3]; these residues are expected to perform structural, substrate-binding, and/or catalytic roles common to the entire FDBR family. Because FDBRs vary in their substrate reduction regiospecificities, we hypothesized that either of these conserved acidic residues might function to protonate the bilin substrate on the pyrroleninic nitrogen of ring B/C (Fig. 1). Other residues conserved exclusively in the PcyA subfamily include histidine 71 (His^{71}), histidine 85 (His^{85}), cysteine 86 (Cys^{86}), cysteine 210 (Cys^{210}), and lysine 218 (Lys^{218}). Such residues therefore are good candidates for a PcyA-specific function such as exovinyl reduction. Using a combination of chemical modification and site-directed mutagenesis, the present work was undertaken to probe the involvement of these conserved residues in PcyA-mediated BV reduction.

EXPERIMENTAL PROCEDURES

Materials—All of the chemicals are American Chemical Society grade or better unless otherwise specified. Diethylpyrocarbonate (DEPC; cat. no. 5758), phenylglyoxal (cat. no. P-7013), 5,5′-dithiobis-2-nitrobenzoic acid (DTNB; cat. no. D-8130), 2,4,6-trinitrobenzenesulfonic acid (TNBS; cat. no. P-2297), NADPH (cat. no. N-1630), ferredoxin:

* This work was supported by USDA Grant 2004-02962 (to J. C. L.) and National Institutes of Health Grant GM073789 (to R. D. B.). The costs of publication of this article were defrayed in part by the payment of page charges. This article must therefore be hereby marked "*advertisement*" in accordance with 18 U.S.C. Section 1734 solely to indicate this fact.

[1] To whom correspondence should be addressed: Section of Molecular and Cellular Biology, College of Biological Sciences, University of California, Davis, CA 95616. Tel.: 530-752-1865. E-mail: jclagarias@ucdavis.edu.

[2] The abbreviations used are: FDBR, ferredoxin-dependent bilin reductase; PCB, phycocyanobilin; BV, biliverdin IXα; 18^1,18^2-DHBV, 18^1,18^2-dihydrobiliverdin IXα; BVH^+, *N*-protonated biliverdin IXα; 18^2-MHBVH$^+$, *N*-protonated 18^2-monohydrobiliverdin IXα radical cation; 18^1,18^2-DHBVH$^+$, *N*-protonated 18^1,18^2-dihydrobiliverdin IXα; 2,18^1,18^2-THBVH$^+$, *N*-protonated 2,18^1,18^2-trihydrobiliverdin IXα radical cation; Fd, ferredoxin; FNR, ferredoxin:$NADP^+$ oxidoreductase; PcyA, phycocyanobilin:ferredoxin oxidoreductase; HPLC, high pressure liquid chromatography; TES, 2-[2-hydroxy-1,1-bis(hydroxymethyl)ethyl]aminoethanesulfonic acid; DEPC, diethylpyrocarbonate; TNBS, 2,4,6-trinitrobenzenesulfonic acid; DTNB, 5,5′-dithiobis-2-nitrobenzoic acid; NIR, near infrared.

[3] Residue numbering corresponds to the *Nostoc* sp. PCC7120 PcyA protein.

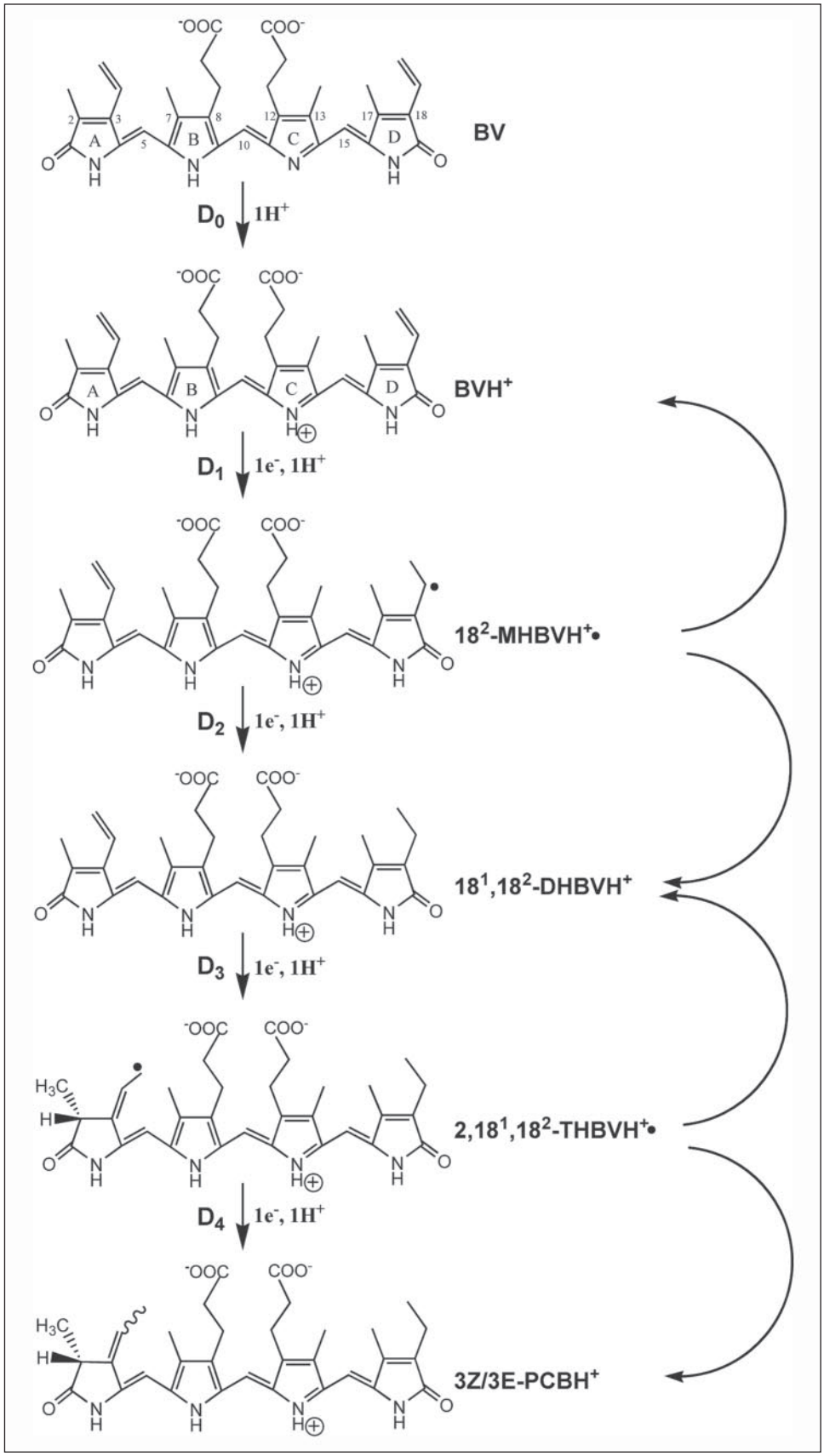

FIGURE 1. **Reaction scheme for PcyA catalysis.** Based on previous studies, PcyA-mediated BV reduction was proposed to involve four sequential proton-coupled electron transfers to the fully *N*-protonated, PcyA-bound substrate (6). Proposed proton-donating residues in the enzyme include: D_0 for protonation of the B- or C-ring nitrogen of BV; D_1 for protonation of C-18^2 position of BVH^+ during the first electron transfer; D_2 for protonation of C-18^1 position of 18^2-$MHBVH^{\ddagger}$ during the second electron transfer; D_3 for protonation of the C-2 position of 18^1,18^2-$DHBVH^+$ during the third electron transfer; and D_4 for protonation of the C-3^2 position of 2,18^1,18^2-$THBVH^{\ddagger}$ during the third electron transfer to yield 3Z/3E-PCB product. The disproportionation reactions observed for each radical intermediate are indicated by the *curved arrows*.

$NADP^+$ oxidoreductase (FNR; cat. no. F-0628), glucose oxidase (cat. no. G6125), catalase (cat. no. C-40), and glutathione-agarose (cat. no. G4510) were purchased from Sigma-Aldrich. Bovine serum albumin (cat. no. 100-018) was purchased from Roche Applied Science. Superdex^{TM} 200 gel filtration matrix, expression vector pGEX-6P-1, and PreScission^{TM} protease were purchased from Amersham Biosciences.

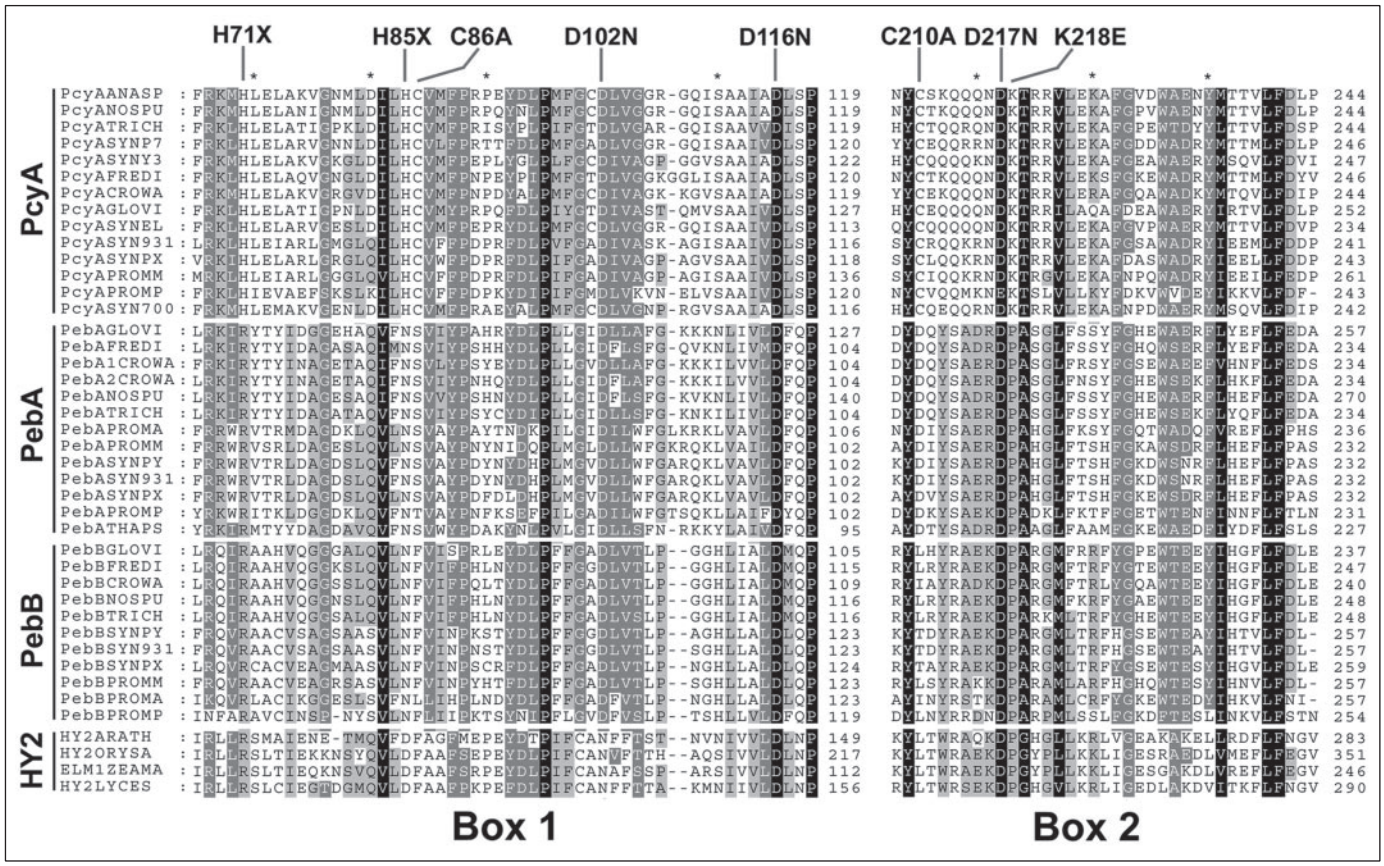

FIGURE 2. **Multiple sequence alignment of the FDBR family.** Partial multiple sequence alignments of PcyA, PebA (15,16-dihydrobiliverdin:ferredoxin oxidoreductase, EC 1.3.7.2), PebB (phycoerythrobilin:ferredoxin oxidoreductase, EC 1.3.7.3), and HY2 (phytochromobilin synthase or phytochromobilin:ferredoxin oxidoreductase, EC 1.3.7.4), members of the FDBR family, were constructed using ClustalW, MEME, and GENEDOC (2). Sequence similarity groups (D = E, K = R, F = Y = W, L = I = V = M, and A = S = T = *p* = G) were used to highlight identity among 100% (*white letters* on *black background*), 80% (*white letters* on *gray background*), and 60% (*black letters* on *gray background*) of the sequences shown. *Nostoc* sp. PCC7120 PcyA sequence numbers are indicated for sites targeted for mutation in this study. *Numbers* on the *right* of each region correspond to the actual sequence numbers for that species. *Box 1* and *Box 2* refer to two highly conserved regions of FDBRs.

HPLC-grade acetone, acetonitrile, formic acid, and spectroanalytical grade glycerol were obtained from Fisher. Ultrafree-4 concentrators were purchased from Millipore Corp. Sep-Pak Light cartridges were obtained from Waters (cat. no. WAT023501). BCA protein assay reagents were purchased from Pierce (cat. no. 23228). Biliverdin IXα (BV) was prepared as described previously (7).

Site-directed Mutagenesis, Protein Expression, and Purification—Expression and purification of wild type recombinant *Nostoc* sp. PCC7120 PcyA were performed as described previously (5). All site-directed mutants were generated in pGEX-*pcyA* using the QuikChange site-directed mutagenesis kit (Stratagene). Glutathione *S*-transferase-tagged PcyA mutant proteins were expressed and purified using a method similar to wild type with the following modification. For mutant protein expression, *Escherichia coli* strain DH5α containing mutant plasmid constructs were grown at 37 °C in 500-ml batches of Luria-Bertani medium containing ampicillin (100 μg/ml) to an A_{600} of 0.6–1.0. Cultures were induced by the addition of 0.1 mM isopropyl thio-β-galactoside and incubated for an additional 4 h at 20 °C, and bacteria were harvested subsequently by centrifugation. Recombinant *Synechococcus* sp. PCC7002 ferredoxin (Fd) was purified as described previously (8). Purified Fd was dialyzed against TKK buffer (25 mM TES-KOH, pH 8.5, and 100 mM KCl). Both PcyA and Fd preparations were flash-frozen in liquid nitrogen and stored at −80 °C prior to use.

Chemical Modification of PcyA—For cysteine- and lysine-selective modification, 20 μM PcyA was incubated with various concentrations of DTNB in 0.1 M Tris-HCl, pH 7.5, or TNBS in 0.1 M phosphate, pH 8.0, at 22 °C for 10 min (9). Reaction mixtures were quenched with excess glutathione for DTNB and Tris-HCl for TNBS. For substrate protection, equimolar BV was mixed with PcyA for 10 min prior to incubation with the chemical reagent. For histidine-selective modification, 20 μM PcyA in 0.1 M phosphate buffer, pH 6.0, was incubated with various concentrations of freshly prepared ethanolic solutions of DEPC at 22 °C. Final concentrations of ethanol never exceeded 1% of the sample volume; control experiments with this amount of ethanol showed no affect on activity. At various times, samples were aliquoted and quenched with 10 mM histidine, and residual PcyA activity was determined. For substrate protection, an equal molar ratio of BV to PcyA was mixed for 10 min prior to DEPC inactivation. Reactivation of DEPC-inactivated enzyme with hydroxylamine was assessed by first incubating 20 μM PcyA in 0.1 M phosphate buffer, pH 6.0, with 0.4 mM DEPC for 10 min at 22 °C until enzyme activity decreased to 15% of its original activity. The reaction was quenched with 10 mM histidine. Hydroxylamine was then added to a final concentration of 0.5 M using stock solution of hydroxylamine that was adjusted to pH 7.0 with NaOH. Aliquots were removed after incubation for 6 h, and residual enzyme activity was measured. Control reactions using unmodified enzyme were similarly performed, indicating that hydroxylamine treatment did not affect enzyme activity.

PcyA Enzyme Assay—PcyA steady state assays were performed similarly to those described previously with minor modifications (5). Standard assay conditions consisted of 25 mM TES-KOH, pH 8.5, 100 mM KCl, 0.025 unit/ml FNR, 5 μM Fd, 100 μM bovine serum albumin, 10 μM BV, 0.1 μM purified wild type or mutant PcyA, 25 units/ml glucose

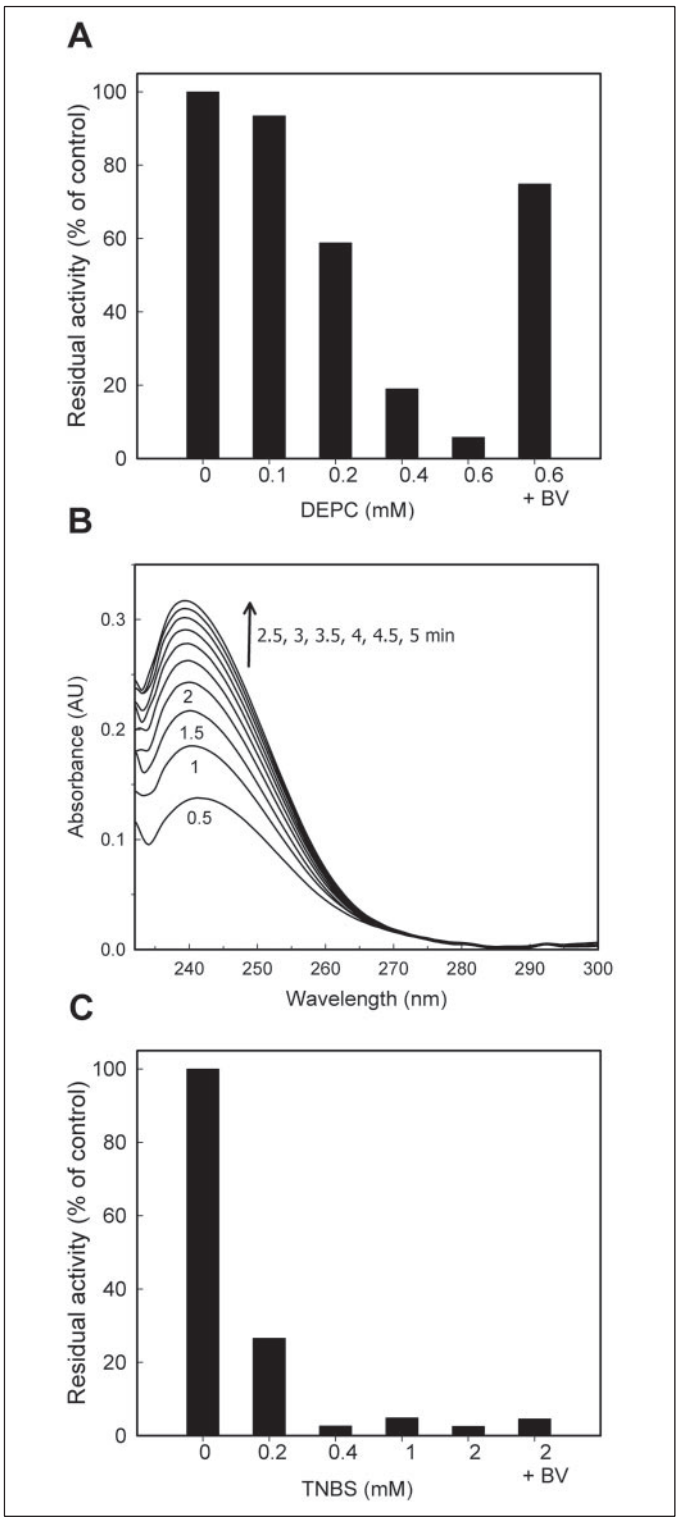

FIGURE 3. **Chemical modification of PcyA.** *A*, chemical inactivation and substrate protection studies. PcyA (20 μM) was incubated with various concentrations of DEPC in 0.1 M phosphate, pH 6.0, at 22 °C for 10 min. For substrate protection experiments, 20 μM BV was preincubated with PcyA. After incubation, reaction mixtures were quenched by the addition of excess of histidine followed by steady state PcyA assays and HPLC analysis performed as described under "Experimental Procedures." Integrated peak areas *versus* time were plotted as described previously (6). *B*, PcyA (20 μM) was incubated with 0.4 mM DEPC in 0.1 M phosphate, pH 6.0. Absorption spectra were recorded at various time intervals as indicated. *C*, inactivation of PcyA activity by TNBS. PcyA (20 μM) was incubated with various concentrations of TNBS in 0.1 M phosphate, pH 8.0, at 22 °C for 10 min. For substrate protection experiments, 20 μM BV was preincubated with PcyA. A standard bilin reductase assay and HPLC analysis were performed after incubation. Integrated peak areas of reaction product 3Z and 3E-PCB in HPLC profiles were plotted.

oxidase, 100 mM glucose, and 25 units/ml catalase. Excess NADPH (*i.e.* 30 μM) was added to initiate catalysis. Reaction mixtures were incubated at 30 °C for 20 min (previously determined to be within the linear range for PcyA activity (6)). Crude bilins were extracted with a Sep-Pak C_{18} light cartridge and subsequently evaporated to dryness using a SpeedVac concentrator. HPLC analysis and anaerobic single-turnover PcyA assays were performed as described previously (6).

Spectroscopic Measurements—Absorption and EPR spectroscopic measurements were performed as described previously (6). For EPR measurements, the anaerobic assay was used with the exception that concentrations of PcyA, BV, and FNR were all increased 4-fold (to 40 μM, 40 μM, and 12 nM, respectively), and 15% spectroanalytical grade glycerol was included in the reaction mixtures. At various time points after the addition of NADPH, absorption spectra were recorded, and 200-μl aliquots were withdrawn from reaction mixtures, transferred to 4-mm quartz EPR tubes, and immediately frozen in liquid nitrogen. Continuous wave EPR studies of PcyA were performed using a Bruker ECS106 spectrometer. EPR spectra at 15 K were acquired using the X-band microwave frequency of 9.69 GHz with modulation amplitude of 4 G. The temperature of the sample was maintained using an Oxford ESR900 liquid helium cryostat and an Oxford ITC 503 temperature controller.

RESULTS

Sequence Alignment of PcyA Family Members Suggests Candidate Proton Donors—Previous functional genomic analysis has identified more than 30 FDBRs in different organisms (2). A multiple sequence alignment implicates the structural and functional significance of two highly conserved regions of the FDBR family (Fig. 2, *Boxes 1* and *2*). Of note are several conserved ionizable residues that are present in these regions. Among the conserved residues, histidine and cysteine residues initially were considered good candidates for D_1 and D_2 proton donors (Fig. 1) because of their exclusive occurrences in the PcyA family (Fig. 2), the near neutral range of their pK_as, and the possibility that they would be protonated upon initial BV substrate binding. For this reason, histidine- and cysteine-selective chemical modification experiments were undertaken.

Chemical Modification Experiments Implicate a Catalytic Role for Histidine Residues—The histidine-selective modification reagent DEPC was chosen for the initial investigation. PcyA and preformed PcyA·BV complexes were treated with increasing concentrations of DEPC, and residual activity was determined. DEPC treatment reduced PcyA activity to less than 20% of mock-treated enzyme within 10 min at a modifier-to-enzyme molar ratio of 20 to 1, implicating the participation of a histidine residue(s) in the catalytic cycle (Fig. 3*A*). The observation that DEPC-inactivation could be prevented by the presence of BV substrate (Fig. 3*A*) demonstrated that one or more sensitive histidine residues of PcyA are protected upon substrate binding, consistent with a direct role for histidine(s) in the PcyA catalytic mechanism. Although DEPC selectively modifies the imidazole side chain of histidine, it can also react with other nucleophilic groups including the amino terminus as well as the side chains of cysteine, tyrosine, lysine and arginine residues (9). The possibility that DEPC inactivates PcyA through arginine and cysteine modification was ruled out because both phenylglyoxal and DTNB, modifying reagents selective to these amino acid residues, had no effect on PcyA activity (data not shown). The reaction of DEPC with tyrosine is typically accompanied by a decrease in absorbance at 275 to 280 nm due to the *O*-carboxyethylation (9). As shown in Fig. 3*B*, DEPC modification of PcyA only revealed an absorbance increase at 240 nm due to carboxyethylation of the histidine imidazole side chain. This result sug-

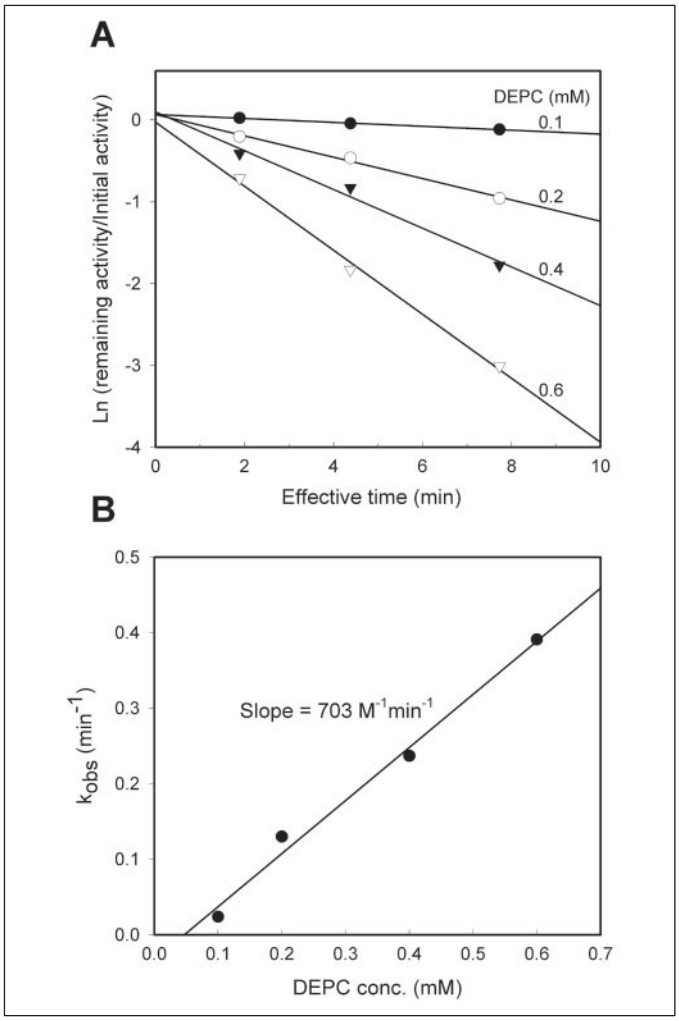

FIGURE 4. **Inactivation of PcyA by DEPC.** *A*, time- and concentration-dependent inactivation of PcyA activity by DEPC. PcyA (20 μM) in 0.1 M phosphate, pH 6.0, was incubated with 0.1 mM (*filled circles*), 0.2 mM (*open circles*), 0.4 mM (*filled triangles*), or 0.6 mM (*open triangles*) DEPC at 22 °C. Samples were withdrawn at various time intervals to determine residual activities. Inactivation data were fitted to the equation $\ln(A/A_0) = -(k/k')I_0(1 - e^{-k't})$ to obtain the pseudo-first-order rate constants of inactivation. *B*, plot of the concentration dependence of k_{obs} for the inactivation of PcyA activity.

gests the DEPC inactivation is not due to the modification of tyrosine residues. Treatment of DEPC-inactivated PcyA with hydroxylamine resulted in only partial recovery of PcyA activity (*i.e.* from 16% (+DEPC) residual activity to 59% (+DEPC, +hydroxylamine); data not shown). This result suggested that DEPC may have modified structurally and/or functionally important lysine residues, because hydroxylamine cannot cleave carboxyethyl adducts from lysine. Indeed, the strong inactivation of PcyA activity by TNBS (Fig. 3) suggests that the modifiable lysine residue(s) are easily accessible to chemical modification. In contrast to the results for DEPC, TNBS inactivation was not prevented by the presence of BV substrate, suggesting that the lysine residues critical for PcyA function are located on the protein surface (Fig. 3*C*). Taken together, these results indicate the importance of both histidine and lysine residues in catalysis.

To probe the role of histidine more fully, time courses of PcyA inactivation with increasing concentrations of DEPC were examined (Fig. 4). Because DEPC undergoes hydrolysis in aqueous solution, the inactivation process was corrected for the decomposition of DEPC as described by the equation $\ln(A/A_0) = -(k/k')I_0(1 - e^{-k't})$, where A/A_0 is the residual activity at time t, k is the second-order rate constant for

TABLE 1

Relative activities of PcyA wild type and site-directed mutants

Steady state bilin reductase assays were performed as described under "Experimental Procedures." Integrated peak areas of 3Z/3E-PCB reaction products from HPLC profiles were determined as a percentage of those of wild type PcyA. Mutants of nonconserved histidine residues (His[14], His[29], His[31], His[38], His[121], His[184], and His[207]) were all fully active and are not shown below.

Mutant groups	Proteins	Activity
		% of wild type
Wild type	PcyA	100
His mutants	PcyA(H85A)	<1
	PcyA(H85N)	<1
	PcyA(H85Q)	5
	PcyA(H85D)	<1
	PcyA(H85E)	5
	PcyA(H71A)	<1
	PcyA(H71N)	46
	PcyA(H71Q)	65
	PcyA(H71D)	28
	PcyA(H71E)	50
Asp mutants	PcyA(D102N)	11
	PcyA(D116N)	11
	PcyA(D217N)	87
Cys mutants	PcyA(C86A)	90
	PcyA(C210A)	90
Lys mutant	PcyA(K218E)	20

the inactivation of PcyA by DEPC, k' is the pseudo-first-order rate constant for the spontaneous hydrolysis of DEPC, and I_0 is the initial concentration of DEPC (10). Plots of the natural log of residual activity against effective time, $(1 - e^{-k't})$, at various DEPC concentrations yielded linear decay, indicating the inactivation process obeys pseudo-first-order kinetics (Fig. 4*A*). The values for pseudo-first-order rate constants k_{obs} were obtained from the slopes of the linear plots in Fig. 4*A*. A second-order rate constant (k_{inact}) of 703 M^{-1} min^{-1} was obtained from the slopes of the plots of k_{obs} *versus* DEPC concentration (Fig. 4*B*). These results demonstrate that DEPC inactivation of PcyA is a simple bimolecular process, with modification of a single (histidine) residue per enzyme molecule sufficient to cause loss of activity.

Site-directed Mutagenesis Identifies Catalytic Roles for His[85], Asp[102], and Asp[116]—The results from chemical modification experiments implicated a potential catalytic role for one or more histidine residues. To identify specific histidine residue(s) of catalytic importance, all nine histidine residues on PcyA were individually mutagenesized to glutamine. The choice of histidine-to-glutamine substitutions was based on the fact that glutamine retains the hydrogen-bonding ability of histidine but is unable to function as a proton donor. All nine histidine mutants could be purified to homogeneity with similar protein yields to wild type PcyA and retained the ability to bind BV, indicating that none of the histidine residues were essential for protein folding. Steady state PcyA assay measurements revealed wild type activity for all histidine-to-glutamine mutants except for H71Q and H85Q, which retained 65 and 5% activity, respectively, relative to wild type PcyA (Table 1). These "relative activity" measurements were all performed under identical conditions using saturating reductant and a BV substrate concentration in great excess of the apparent K_m, estimated to be in the nanomolar range for the wild-type enzyme, so that the rate of product formation was linear throughout the assay period. Although these assays do not yield quantitative kinetic constants, they were performed to identify potential mutations for more detailed pre-steady state spectroscopic measurements.

To address the catalytic importance of His[71] and His[85], residues conserved in all know PcyA representatives (Fig. 2), additional amino acid substitution mutants were constructed for both residues. Substitution of both residues with alanine effectively abolished all PcyA enzymatic activity, indicating their structural or functional significance. However,

more conservative His[71] mutations, including H71N, H71D, H71Q, and H71E, retained partial activity (Table 1). By contrast, similar mutations of His[85] afforded nearly complete loss of activity (Table 1). Taken together, these results support a catalytic role for His[85] but not for His[71].

With regard to the possible catalytic role for lysine implied by the TNBS experiments, only a single lysine residue is conserved in all members of the PcyA subfamily (Fig. 2). Replacement of this conserved lysine (Lys[218]) with glutamic acid failed to abolish the activity of the enzyme, although the 28EK1 mutant retained only 20% of wild type activity (Table 1). In view of this observation, the results from TNBS modification experiments can better be rationalized by the participation of TNBS-modifiable lysine residue(s) in the electrostatic interaction between PcyA and reduced Fd, an interaction critical for the activity of other Fd-dependent enzymes (11–15). We believe that it is less likely that Lys[218] plays a direct proton-donating role for PcyA-mediated bilin reduction.

In addition to lysine and histidine mutants of PcyA, we also mutagenesized several conserved aspartate (Asp[102], Asp[116], and Asp[217]) and cysteine (Cys[86] and Cys[210]) residues (Table 1). D217N, C86A, and C210A mutants all retained roughly 90% catalytic activity, casting strong doubt that these residues participate in the proton-coupled electron transfer process. Because Asp[217] is universally conserved in the FDBR family, the retention of activity of the D217N mutant was unexpected. By contrast with the Asp[217] and the two cysteine mutants, D102N and D116N mutants were both poorly active, retaining only 11% of wild type activity. These results suggest that Asp[102] and Asp[116] are potentially proton donors during the PcyA catalytic cycle.

Absorption and EPR Measurements Support the Presence of a Catalytic His[85]-Asp[102] Pair for Exovinyl Reduction—To further characterize the functions of His[85] and Asp[102], we compared the spectral properties of the binary BV complexes with wild type and mutant PcyA proteins. Previous studies in our laboratory established that PcyA-bound bilin substrates possess cyclic, porphyrin-like conformations (5, 6). In those studies, we showed that BV binding to apoPcyA is accompanied by an absorbance increase at 650 nm that mirrors the more constrained geometry of the bound bilin. In addition to this absorbance enhancement, we also observed the appearance of a near infrared (NIR) absorbing species that was attributed to the protonated PcyA-bound form of BV (6). It was reasoned that the formation of the protonated bilin would favor electron transfer, conceivably by raising its midpoint potential for reduction. In this regard, no NIR absorbing species was observed for bilin analogs that were poor substrates for PcyA (5, 6).

Spectroscopic comparison of the four His[85] mutants revealed that only H85Q retained the ability to bind BV based upon the characteristic absorption increase at 650 nm (Fig. 5, *top panel*), whereas the H85N, H85D, and H85E mutants did not (data not shown). These results suggest that the size and/or structure of this residue is critical for bilin binding. Interestingly, the absorption spectrum of the BV complex of H85Q lacked the NIR absorbing species present in the wild type PcyA·BV complex (Fig. 5, *top panel*). To examine the possibility that the H85Q mutant could still support initial electron transfer, we compared the ability of wild type and mutant enzymes to support production of a PcyA-bound bilin radical intermediate. Addition of 1 electron equivalent of NADPH to BV complexes of both proteins led to absorbance increases at 470 and 770 nm, although the extent of the increase was smaller for the H85Q mutant (Fig. 5, *middle two panels*). The absorbance increase for the H85Q mutant eventually reached a maximum that was not followed by the subsequent decay seen for the wild type enzyme. These results are consistent with the interpretation that the H85Q mutant can support formation of a exovinyl bilin radical intermediate

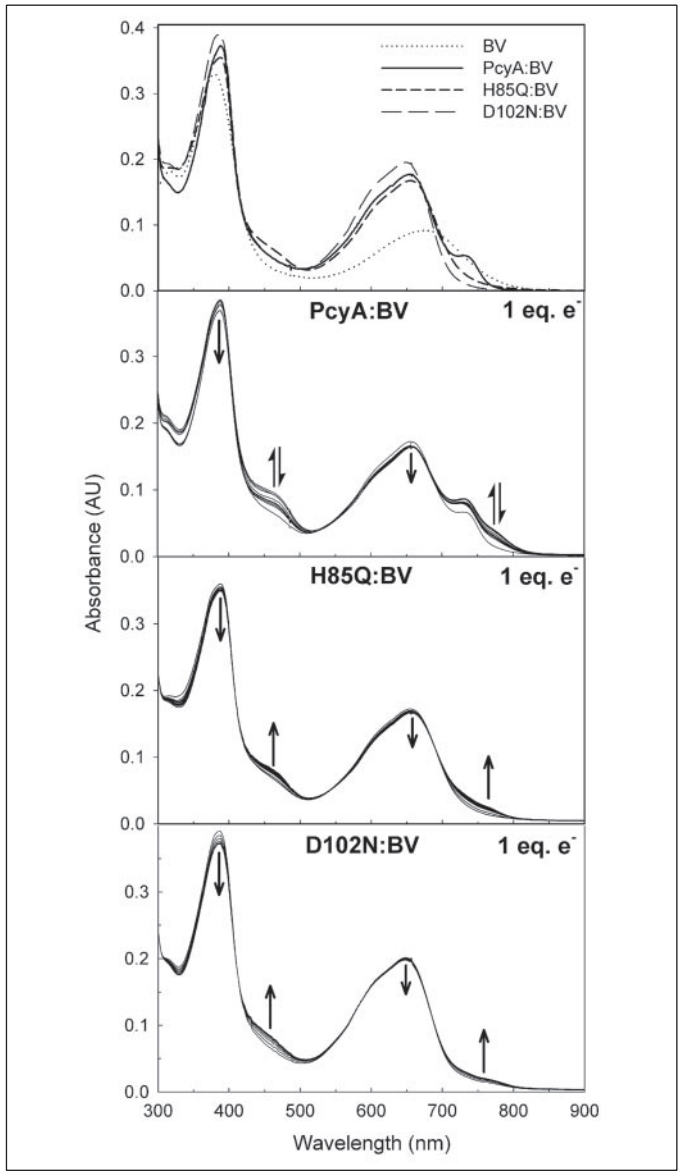

FIGURE 5. **Absorption spectra of BV complexes of wild type PcyA, H85Q, and D102N mutants before and after addition of 1 electron equivalent.** In the *top panel*, the absorption spectra of BV (10 μM) incubated with 10 μM wild type PcyA, H85Q, or D102N mutant proteins at 22 °C for 5 min are compared with the spectrum of 10 μM BV in the same buffer. In the *bottom three panels*, time courses of BV reduction, monitored spectrophotometrically at 1-min intervals, are shown following the addition of 1 molar electron equivalent of reductant (*i.e.* 5 μM NADPH) to samples consisting of 10 μM PcyA·BV, H85Q·BV, or D102N·BV complexes and 3 nM FNR, 10 μM Fd, and an oxygen-scavenging system. Absorbance increases followed by decays at 470 and 770 nm in wild type PcyA reaction are indicated by *double arrows*, and absorbance decreases at 380 and 650 nm in all reactions and increases at 470 and 770 nm in H85Q and D102N reaction are indicated by *single arrows*.

that is stable to disproportionation to BV and 18[1],18[2]-DHBV as is also seen for wild type PcyA (Fig. 1). A similar line of investigation was performed with the D102N mutant. The D102N mutant also yielded a BV complex that lacked the NIR absorbing species and could be converted to a stable exovinyl bilin radical with spectral properties nearly indistinguishable from those of the H85Q mutant (Fig. 5, *bottom panel*). Taken together, these experiments indicate that His[85] and Asp[102] are both essential for exovinyl reduction of BV.

The reduced amount of radical formation observed for the H85Q and D102N mutants suggested that the midpoint potential for BV reduction was lowered in the two mutants. Because the midpoint potential of Fd is

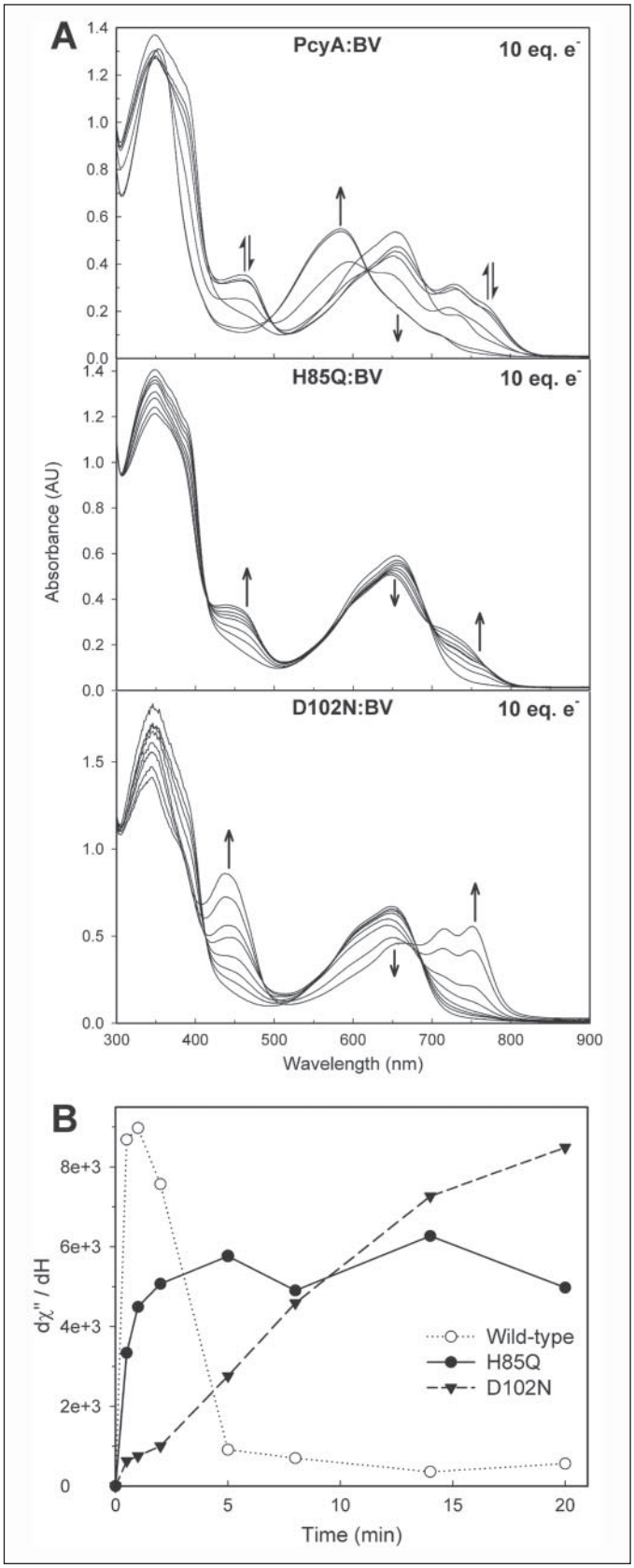

FIGURE 6. **Absorption and EPR spectroscopy of BV complexes of wild type PcyA, H85Q, and D102N mutants after addition of 10 electron equivalents.** *A*, time courses of BV reduction monitored spectrophotometrically at 0, 0.5, 1, 2, 5, 8, 14, and 20 min after the addition of 10 molar electron equivalents of reductant (*i.e.* 200 μM NADPH) to samples containing 40 μM preformed PcyA·BV (*top panel*), H85Q·BV (*middle panel*), and D102N·BV (*bottom panel*) complexes were obtained as described previously (6). Absorbance increases followed by decays at 470 and 770 nm in wild type PcyA reaction are indicated by *double arrows*, and absorbance decreases at 650 nm in all reactions and increases at 470 and 770 nm in H85Q and D102N reaction are indicated by *single arrows*. The absorbance increase at 585 nm in wild type PcyA reaction (indicated by *single arrow*) represents the formation of PCB product. The peak around 340 nm that overlapped with the blue absorption maximum of BV corresponds to NADPH absorption. *B*, EPR measurement of bilin radicals produced during catalysis for wild type PcyA, H85Q, and D102N mutants. For EPR measurements, 200-μl aliquots were withdrawn at 0, 0.5, 1, 2, 5, 8, 14, 20 min after NADPH addition and were immediately frozen in liquid nitrogen. EPR spectra at 15 K were recorded at 9.69 GHz. The intensity of EPR signals was calculated from the sum of peak high and trough depth.

more negative than that of NADPH, we reasoned that increasing the NADPH concentration by a factor of 10 would enhance the yield of the primary PcyA·BV radical. Indeed, we observed increases in both rate and yield of radical formation for the two mutants when 10-fold excess NADPH was added (Fig. 6*A*). Moreover, neither mutant yielded significant quantities of 18^1,18^2-DHBV or PCB under these conditions, whereas wild type PcyA was able to fully convert the BV substrate to PCB (data not shown). These analyses indicate that H85Q and D102N mutants both support initial electron transfer but do not permit the second electron transfer to produce the fully reduced 18^1,18^2-DHBV intermediate depicted in Fig. 1. It is interesting that the spectroscopic properties of the H85Q and D102N bilin radicals are different, with the latter possessing more enhanced NIR absorption (Fig. 6*A*). This result suggests that the chemical structure and/or environment of the two bilin radicals are distinct.

To ascertain that the absorption changes observed during H85Q and D102N reactions correspond to radical intermediates, we performed EPR measurements on freeze-quenched samples. Aliquots were removed at different time points after the addition of NADPH, frozen in liquid nitrogen, and analyzed by EPR spectroscopy at 15 K. Both mutants yielded an isotropic EPR signal at $g \approx 2$ with a peak to trough width of 15 G identical to the EPR signal of the exovinyl radical intermediate for wild type (6). For both mutants, the EPR signal appeared with slower initial rates compared with wild type PcyA (Fig. 6*B*). The kinetics of the radical signal formation was the slowest for the D102N mutant, which continued to increase beyond 20 min and eventually leveled out after 60 min. The appearance of the EPR signals mirrored the absorption changes for all three proteins, indicating that the two spectroscopic signatures corresponded to the formation of a bilin radical (data not shown). Unlike wild type PcyA, in which the EPR signal increased and rapidly decayed, both mutants yielded stable radicals, as their EPR signal intensities showed no evidence for subsequent decay (Fig. 6*B*). Taken together, these results are consistent with a direct role of the His^{85}-Asp^{102} pair in exovinyl reduction of BV.

DISCUSSION

We previously proposed a catalytic mechanism for PcyA involving multiple proton-donating residues in the enzyme that assist the reduction of both exo- and endovinyl groups of BV (6). Through chemical modification and site-directed mutagenesis, we have identified a histidine-aspartate pair, *i.e.* His^{85} and Asp^{102}, required for the initial exovinyl reduction of BV. Our studies also support important roles for Asp^{116} and Lys^{218} in the overall PcyA-mediated conversion of BV to PCB. In the following discussion, we outline the mechanistic implications of these results to provide the conceptional basis for further investigation of this interesting enzyme.

Mechanistic Implications for Substrate and Cofactor Binding—The conclusion that BV binds to PcyA in a constrained, cyclic, "porphyrin-like" conformation is supported by previous spectroscopic measurements (5, 6). BV substrate binding is accompanied by an absorbance increase at 650 nm and by narrowing of the absorption envelope, both of

which can be attributed to decreased mobility of the bound bilin. In addition, PcyA-bound BV possesses enhanced NIR absorption, which previously was attributed to the partial formation of a *N*-protonated substrate (6). In that study, we proposed that a universal proton donor (D_0) with a carboxylic acid side chain is responsible for this spectroscopic signature, because a carboxylate negative charge would stabilize the resulting bilin cation (Fig. 1). We also hypothesized that the D_0 residue would be conserved in the entire FDBR family, because it would favor bilin reduction by stabilizing its protonated form (6). Among the carboxylate-containing amino acid residues of the FDBR family, only Asp^{116} and Asp^{217} are universally conserved. Analysis of the D116N and D217N mutants of PcyA indicates that the ability of either residue to donate a proton and/or to form a carboxylate anion is not required for BV binding. The D217N mutant was nearly as active as wild type PcyA, demonstrating that the acid-base properties of Asp^{217} are not critical for substrate binding or catalysis. The strongly reduced activity of the D116N mutant suggests that the acid-base properties of a carboxylic acid at this position are important for catalysis. Moreover, the BV complex of D116N also lacked the NIR absorption seen in wild type PcyA (data not shown). Although consistent with a requirement for Asp^{116} to protonate and/or stabilize the protonated form of the bilin substrate, the residual activity of the D116N mutant argues against its assignment to D_0. We therefore propose an alternate role(s) for Asp^{116} such as regulating the orientation/pK_a of the primary proton donor D_1, optimizing bilin substrate positioning/affinity, or facilitating product release. Experimental assessment of these possibilities is beyond the scope of the present investigation.

Bilin substrate binding to PcyA is likely to involve ionic interactions between the propionate groups of BV and cationic residues on PcyA. This hypothesis is supported by the observation that uncharged BV methyl ester and amide analogs have reduced binding affinity to PcyA.[4] As Lys^{218} is found in all members of the PcyA subfamily, we considered the possibility that it plays a direct role in BV binding. Although TNBS modification experiments show no protection by BV substrate binding, these experiments do not rule out a role of Lys^{218} in BV substrate binding *a priori*. Indeed, the residual activity of the K218E mutant is significantly decreased, a result consistent with this hypothesis. In view of the lack of substrate protection, however, we favor the interpretation that Lys^{218} governs the electrostatic interaction between PcyA and its Fd cofactor. The importance of a positively charged "docking" surface for reduced Fd has been reported for other Fd-dependent enzymes, *e.g.* FNR, nitrite reductase, and sulfite reductase (11, 12, 14, 16). Because of the high K_m values for wild type FDBRs, however, *i.e.* 4 μM for phytochromobilin synthase (17), we have not experimentally addressed the importance of Lys^{218} in the Fd-PcyA binding affinity at the present time.

Mechanistic Implications for Exovinyl Reduction—Four sequential proton-coupled electron transfers are required to accomplish reductions of both vinyl groups of BV. Previous studies have established that exovinyl reduction precedes endovinyl reduction (5). In that study, we envisaged four proton-donating residues, D_1–D_4, to mediate these electron/proton transfer steps (Fig. 1). D_1 and D_2 residues are the proton donors for exovinyl reduction, which is a PcyA-specific reaction. These residues therefore would not have to be universally conserved in the FDBR family but would have to be present in all PcyA subfamily members. Replacement of D_1 with a residue incapable of proton transfer would be expected to abolish exovinyl reductase activity. Our mutagenesis and spectroscopic studies implicate His^{85} as D_1. In this regard, all four His^{85} mutants examined retain almost no enzymatic activity. With the exception of the H85Q mutant, the His^{85} mutants also poorly bind BV substrate. The absence of the NIR absorption maximum for the BV complex of H85Q mutant supports the hypothesis that H85 also functions to protonate the bilin substrate. On the basis of these results, we conclude that His^{85} participates in substrate binding via its hydrogen-bonding ability and serves as the primary proton donor D_1 for exovinyl reduction.

The observation that the H85Q mutant can support formation of a stable, semi-reduced bilin radical suggests that electron transfer can occur without proton transfer. For both wild type PcyA and the H85Q mutant, the EPR-detected radical signal intensities mirror the appearance of new optical spectroscopic features upon addition of reductant (Figs. 5 and 6). Assuming the redox potentials are equivalent, the wild type radical yield should never exceed that observed for H85Q. This hypothesis is even more compelling because wild type can convert to EPR-silent intermediates that should further reduce its radical signal intensity. Data shown in Fig. 6 reveal that the maximum radical signal intensity for H85Q is considerably less than that observed for wild type at its optimum time point. Because H85Q yields a stable radical, the amount of radical that can be formed at equilibrium will depend upon the concentrations of reduced Fd (10 μM) and the PcyA·BV complex (40 μM) as well as their relative midpoint potentials. The increased amount of wild type PcyA radical produced under the same conditions is therefore consistent with a more positive midpoint potential for wild type PcyA compared with the H85Q mutant.

Similar to the H85Q reaction, the D102N reaction also yields a stable, semi-reduced bilin radical intermediate(s) that remains tightly bound to the enzyme. Radical formation for the D102N reaction is, however, considerably slower than H85Q. In addition, the absorption spectrum of the D102N-bilin radical differs from that of the H85Q reaction, perhaps indicating the formation of a distinct radical species. As judged by EPR and absorption spectra, the D102N reaction ultimately yields more bilin radical than the H85Q reaction. This suggests that the midpoint potential of D102N·bilin complex is more positive than H85Q·bilin complex, albeit still less positive than wild type PcyA·bilin complex. Although there are a number of possible interpretations of these results, we favor the hypothesis that His^{85} and Asp^{102} function as a catalytic dyad for exovinyl reduction depicted in Fig. 7. We envisage a charge-stabilized His^{85}-Asp^{102} pair in the apoPcyA enzyme. Substrate binding is facilitated by formation of a hydrogen bond between the His^{85} imidazolium side chain and the C-19 carbonyl oxygen of BV (**1**). This leads to partial protonation of PcyA-bound BV substrate, which accounts for the NIR absorption maximum of the enzyme·substrate complex. Concomitant with electron transfer, the imidazolium proton is transferred to O-19 of the BV radical anion (**2**), producing the *O*-protonated neutral BV radical (**3**), which ultimately rearranges to the neutral ethylidene radical 18^2-MHBV$^{\bullet}$ (**4**).

As depicted in Fig. 7, this mechanism can account for the loss of activity of the H85Q and D102N mutants. Although the histidine-to-glutamine substitution would be expected to retain the hydrogen bond between O-19 and the amide side chain of glutamine, *O*-protonation and proton transfer would not occur. In addition to lowering the midpoint potential, only the semi-reduced BV radical anion could be formed in the H85Q mutant. The midpoint potential of the D102N·bilin complex would also be expected to be more negative than wild type PcyA·bilin complex, because the H85 imidazole side chain would not be charged (Fig. 7). By comparison with the H85Q mutant, the hydrogen bond between the O-19 carbonyl of BV and the imidazole proton of the D102N mutant would be more similar to that found in the wild type enzyme. Indeed, it is conceivable that some proton transfer occurs from H85 on the D102N mutant to O-19 of the BV radical

[4] L. Shang and J. C. Lagarias, unpublished data.

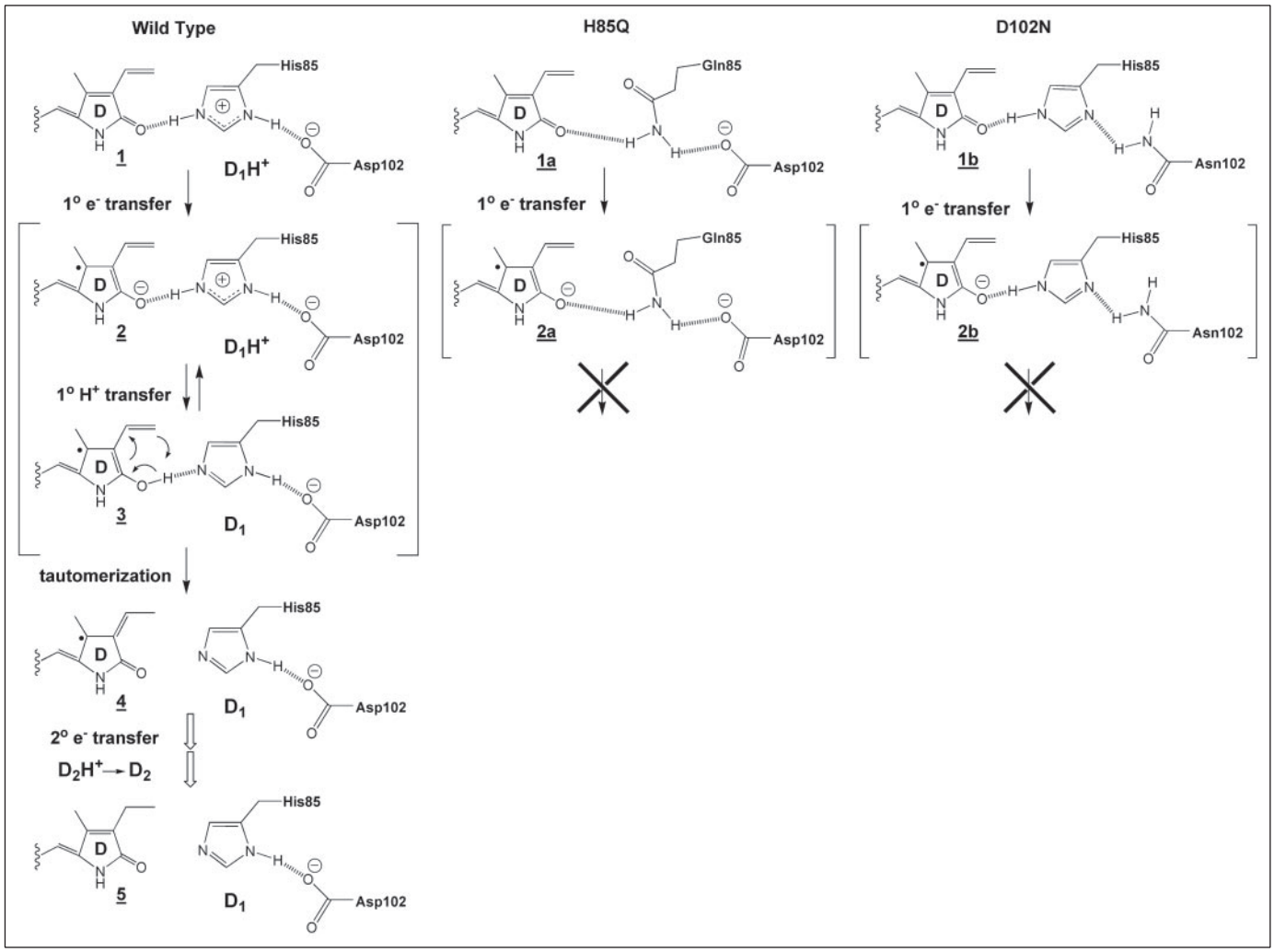

FIGURE 7. **Proposed mechanism for PcyA-catalyzed exovinyl reduction for wild type and site-directed mutants.** For wild type PcyA reaction (*left panel*), the C-19 carbonyl of neutral BV **1** is hydrogen-bonded to the protonated imidazole side chain of His^{85}, which is stabilized by hydrogen-bonding to the carboxylate side chain of Asp^{102}, *i.e.* the His^{85}-Asp^{102} pair corresponds to the primary proton donor D_1H^+. Upon primary electron transfer, proton transfer to the BV radical anion **2** occurs to produce the neutral, O-19-protonated BV radical **3.** Through intramolecular tautomerization, species **3** should readily convert to the C-18^2-protonated BV radical species **4**. Second electron transfer, accompanied by subsequent proton transfer from D_2H^+ (not identified in this study) yields the stable $18^1,18^2$-DHBV intermediate **5**. For H85Q and D102N mutant reactions, primary electron transfer occurs; however, proton transfer is not permitted from the glutamine amide side chain of H85Q (*middle panel*) or from the neutral His^{85} imidazole side chain of the D102N mutant (*right panel*). The hydrogen bonds between the C-19 carbonyl of BV substrate and the residue at position 85 are expected to be considerably stronger for wild type PcyA compared with the two mutants in the order WT > D102N > H85Q. The protein environment of radical anions **2a** and **2b** are different, thus accounting for their dissimilar absorption spectra.

anion that may even rearrange to the ethylidine radical **4**. Either scenario may account for the distinct optical properties of the semi-reduced bilin radicals for the D102N and H85Q mutants (Fig. 6). The stability of the semi-reduced H85Q and D102N bilin radicals, even in the presence of excess reductant, suggests that further O-19 protonation of **4** is required for full exovinyl reduction. We therefore conclude that the His^{85}-Asp^{102} pair may also be responsible for regulating transfer of the second proton to the C-18^1 position to yield the intermediate $18^1,18^2$-DHBV. The present studies do not identify the second proton donor (D_2); however, possibilities include bound solvent or a proton-donating residue in hydrogen-bonding contact with the His^{85}-Asp^{102} pair. With regard to the latter possibility, His^{85} itself could function as D_2 by receiving another proton from a proton relay within the enzyme. Resolution of these issues will be greatly aided by structural information for a member of the FDBR family.

Semi-empirical AM1 calculations previously were used to simulate the absorption spectra of the PcyA·BV complex and the semi-reduced radical species produced upon electron transfer (6). In that study, we hypothesized that their spectra reflect partial protonation of the PcyA-bound bilin substrate/radical. However, it was not possible to discriminate between *N*-protonation and *O*-protonation because of the similarity of their calculated spectra. In view of the proposed role for His^{85} as D_1, we now favor His^{85}-directed protonation of the O-19 carbonyl oxygen atom to account for the NIR absorption signature of the PcyA·BV complex (Fig. 7). The lack of O-19 protonation in the H85Q and D102N reactions is consistent with the absence of this spectral property. Taken together with our inability to identify a universally conserved proton donor D_0 that is essential for PcyA activity, we conclude that bilin substrate protonation reflects distinct residues in the different classes of the FDBR family.

Mutations that permit exovinyl reduction of BV without endovinyl reduction (to yield the intermediate $18^1,18^2$-DHBV) or endovinyl reduction of BV without exovinyl reduction (to yield its isomer phytochromobilin) were not identified by our studies. This suggests that single point mutations may not be able to simultaneously alter the substrate positioning and/or its multiple redox potential(s) in a manner that would enable formation and release of a two electron reduced product. In this regard, the three FDBRs that utilize BV as substrate, PcyA, PebA, and HY2, possess less than 30% sequence identity (2). This suggests that multiple amino acid substitutions may be required to alter the reduction

regiospecificity of PcyA. Because of the limited scope of the present mutagenesis survey, however, it is possible that we have missed single residues that could so alter the reduction regiospecificity of PcyA. With a suitable screening method, a directed evolution approach might be a better approach to address this question.

It is particularly interesting that neither the H85Q or the D102N mutant of PcyA could support full endovinyl reduction, the reaction mediated by phytochromobilin synthase or HY2 (17). However, both His^{85} and Asp^{102} are required for endovinyl reduction, because stable radicals were formed when 18^1,18^2-DHBV was used as substrate for either H85Q or D102N mutant (data not shown). Although it could perform a substrate-positioning role, the His^{85}-Asp^{102} pair might also regulate the midpoint potential for endovinyl reduction via protonation of the D-ring carbonyl.

Future Studies—Although we have identified the initial proton donor D_1 for PcyA-mediated exovinyl reduction in this investigation, considerable experimental work remains to elucidate the overall catalytic mechanism of PcyA. The stable radicals generated for the H85Q and D102N mutants are ideal candidates for advanced EPR studies including ENDOR (electron nuclear double resonance) and ESEEM (electron spin echo envelope modulation) measurements using isotopically labeled BV and its analogs (18). Ultimately, solving the three-dimensional structure of PcyA will be required to advance our understanding of the catalytic mechanism utilized by this novel class of radical enzyme.

Acknowledgments—We thank Dr. Nathan Rockwell, Lixia Shang, and Yi-shin Su for critical reading of the manuscript.

REFERENCES

1. Beale, S. I. (1993) *Chem. Rev.* **93,** 785–802
2. Frankenberg, N., Mukougawa, K., Kohchi, T., and Lagarias, J. C. (2001) *Plant Cell* **13,** 965–978
3. Glazer, A. N. (1999) in *Chemicals from Microalgae* (Cohen, Z., ed) pp. 261–280, Taylor and Francis, London
4. Frankenberg, N. F., and Lagarias, J. C. (2003) in *The Porphyrin Handbook. Chlorophylls and Bilins*: *Biosynthesis Structure and Degradation.* (Kadish, K. M., Smith, K. M., and Guilard, R., eds) Vol. 13, pp. 211–235, Academic Press, New York
5. Frankenberg, N., and Lagarias, J. C. (2003) *J. Biol. Chem.* **278,** 9219–9226
6. Tu, S., Gunn, A., Toney, M. D., Britt, R. D., and Lagarias, J. C. (2004) *J. Am. Chem. Soc.* **126,** 8682–8693
7. Elich, T. D., McDonagh, A. F., Palma, L. A., and Lagarias, J. C. (1989) *J. Biol. Chem.* **264,** 183–189
8. Schluchter, W. M. (1994) *The Characterization of Photosystem I and Ferredoxin-NADP+ Oxidoreductase in the Cyanobacterium Synechococcus sp. PCC 7002.* Ph.D. dissertation, Pennsylvania State University, University Park, PA
9. Lundblad, R. L. (2005) *Chemical Reagents for Protein Modification*, CRC Press, Boca Raton, FL
10. Gomi, T., and Fujioka, M. (1983) *Biochemistry* **22,** 137–143
11. Akashi, T., Matsumura, T., Ideguchi, T., Iwakiri, K., Kawakatsu, T., Taniguchi, I., and Hase, T. (1999) *J. Biol. Chem.* **274,** 29399–29405
12. Dose, M. M., Hirasawa, M., Kleis-SanFrancisco, S., Lew, E. L., and Knaff, D. B. (1997) *Plant Physiol.* **114,** 1047–1053
13. Kurisu, G., Kusunoki, M., Katoh, E., Yamazaki, T., Teshima, K., Onda, Y., Kimata-Ariga, Y., and Hase, T. (2001) *Nat. Struct. Biol.* **8,** 117–121
14. Martinez-Julvez, M., Hermoso, J., Hurley, J. K., Mayoral, T., Sanz-Aparicio, J., Tollin, G., Gomez-Moreno, C., and Medina, M. (1998) *Biochemistry* **37,** 17680–17691
15. De Pascalis, A. R., Jelesarov, I., Ackermann, F., Koppenol, W. H., Hirasawa, M., Knaff, D. B., and Bosshard, H. R. (1993) *Protein Sci.* **2,** 1126–1135
16. Medina, M., Martinez-Julvez, M., Hurley, J. K., Tollin, G., and Gomez-Moreno, C. (1998) *Biochemistry* **37,** 2715–2728
17. McDowell, M. T., and Lagarias, J. C. (2001) *Plant Physiol.* **126,** 1546–1554
18. Prisner, T., Rohrer, M., and MacMillan, F. (2001) *Annu. Rev. Phys. Chem.* **52,** 279–313